Article

Chinese Science Bulletin

Atmospheric Science

November 2013 Vol.58 No.33: 4161–4170
doi: 10.1007/s11434-013-5996-7

Investigation of the consistency of atmospheric CO_2 retrievals from different space-based sensors: Intercomparison and spatiotemporal analysis

WANG TianXing*, SHI JianCheng, JING YingYing & XIE YanHui

State Key Laboratory of Remote Sensing Science, Jointly Sponsored by the Institute of Remote Sensing and Digital Earth, Chinese Academy of Sciences and Beijing Normal University, Beijing 100101, China

Received March 29, 2013; accepted May 24, 2013; published online July 22, 2013

In recent years, global warming caused by emission of CO_2 has attracted considerable attention from the public. Although the measurements from AIRS, GOSAT, SCIAMACHY and IASI have been frequently used to derive atmospheric CO_2 concentration, comprehensive quantification of the differences among these CO_2 products is still not fully investigated yet. In this paper, a series of strategies have been proposed to allow the CO_2 products from different instruments to be physically inter-comparable. Based on this, these CO_2 products are inter-compared in terms of magnitude and their spatiotemporal distributions. The results reveal that the correlations among these CO_2 products are relatively weak, and some discrepancies are detected in terms of the CO_2 spatiotemporal characteristics, demonstrating more efforts should be made in the future to improve the retrievals of CO_2. Their spatial coverage differences reflected in this study imply the great necessity to generate consistent products with improved spatial and temporal continuities by combining these CO_2 measurements.

atmospheric CO_2, AIRS, GOSAT, SCIAMACHY, IASI

Citation: Wang T X, Shi J C, Jing Y Y, et al. Investigation of the consistency of atmospheric CO_2 retrievals from different space-based sensors: Intercomparison and spatiotemporal analysis. Chin Sci Bull, 2013, 58: 4161–4170, doi: 10.1007/s11434-013-5996-7

Carbon dioxide (CO_2) is the most important greenhouse gas produced by human activities, primarily through the combustion of fossil fuels. Its concentration in the Earth's atmosphere has increased from about 280 to 380 ppm over the past century [1]. Global warming induced by atmospheric CO_2 has attracted more and more attention of researchers all over the world. Although traditional ground-based CO_2 measurements have high accuracies and the data are collected in a successive manner at temporal scale, however, the spatial coverage is sparse and even entirely absent in certain areas such as oceans as well as most parts of Polar Regions [2,3]. Thus it is impossible to accurately determine the sources and sinks of CO_2 based solely on ground measurements. Satellite sounders with various spatial, temporal and spectral resolutions provide the unique opportunity to map atmospheric CO_2 globally. Currently the available hyperspectral on-orbit payloads that can be used to retrieve the atmospheric CO_2 include the Atmospheric InfraRed Sounder (AIRS) [4,5], the Infrared Atmospheric Sounding Interferometer (IASI) [6], the SCanning Imaging Absorption spectroMeter for Atmospheric CartograpHY (SCIAMACHY) [7] and the Greenhouse gases Observing SATellite (GOSAT) [8,9]. Generally, the above mentioned sounders can be grouped into two types according to the wavelengths they work on: (1) TIR sounders such as AIRS and IASI which mainly work in thermal infrared spectral region with the maximum sensitivity in the middle to up troposphere; (2) NIR/SWIR sounders such as SCIAMACHY and GOSAT which measure reflected solar radiation in the NIR/SWIR spectral region and the measurements have almost constant sensitivity to the entire atmosphere column with the maximum value near the surface [3,10]. Thus, NIR/SWIR sounders are frequently used to derive the column-averaged dry air mole fractions of CO_2 in the atmosphere (XCO_2). Specially, the

*Corresponding author (email: wangtx@irsa.ac.cn)

GOSAT could also perform measurements in the TIR bands which can be employed to retrieve the atmospheric CO_2 profile. Except for the instruments mentioned above, the second Orbiting Carbon Observatory (OCO-2) as a rebuilt of OCO [11] is also scheduled to launch in late 2014 [3].

Since all the instruments mentioned above operate in the optical spectral region (<16 μm), their abilities to monitor the atmospheric CO_2 are significantly limited by the presence of clouds, moreover, the NIR/SWIR sounders can only collect data during the day time. For instance, work of Morino et al. [1] showed that only about ten percent of GOSAT data can be used for XCO_2 retrieval due to the cloud contaminations. The amount of CO_2 measurements will even be smaller if other screening criteria are further applied (such as quality of the spectral fit, aerosol loadings etc.). Therefore it is desirable to combine the available CO_2 products to produce improved CO_2 datasets and in turn to improve the model predictions of global CO_2 sources and sinks. For this point, on the one hand, it is highly necessary to develop effective strategies to make these CO_2 measurements with different spatial and temporal characteristics to be physically comparable; on the other hand, it is an indispensable step to quantify their differences before jointly using them. This is the main motivation and effort of this paper.

The objectives of this study focus on (1) developing algorithms to spatiotemporally match those available CO_2 products derived from different instruments, aiming to make such CO_2 products to be physically comparable with each other; (2) quantifying the differences among these available CO_2 products in terms of specific CO_2 values as well as spatiotemporal characteristics; and (3) also demonstrating the current retrieval status of atmospheric CO_2 from space.

1 Datasets

1.1 AIRS

AIRS, launched into Earth-orbit on May 4, 2002 on board NASA's Aqua satellite, is designed to measure radiances in the thermal infrared (3.7–15.4 μm) using 2378 channels at a nominal spectral resolution of $\lambda/\Delta\lambda$=1200[4]. AIRS along with AMSU and HSB compose the AIRS/AMSU/HSB sounder system which represents the most advanced atmospheric sounding system ever deployed in space (http://airs.jpl.nasa.gov/mission/description/). During the retrieval, data from one AMSU footprint and nine AIRS footprints are used to create a single "cloud-cleared" infrared spectrum [5]. The operational AIRS CO_2 product is derived using vanishing partial derivatives (VPD) algorithm [12], which is based on AIRS Level 2 physical retrieval products, such as profiles of temperature, water vapor and ozone. Thus, it is namely a post-process product. The current released version of AIRS CO_2 product is v5 with a nominal spatial resolution of 90 km×90 km at nadir (2×2 arrays of AMSU FOVs). It is available at the MIRADOR portal on the NASA Goddard Earth Sciences Data and Information Services Center (GES DISC; http://mirador.gsfc.nasa.gov/).

1.2 GOSAT

GOSAT, as the first space-based sensor designed specifically to accurately measure CO_2 with improved sensitivity and spatial resolution, was successfully launched on 23 January, 2009 [8,9,11]. The observation instrument of GOSAT is composed of two subunits: the Fourier Transform Spectrometer (FTS) and the Cloud and Aerosol Imager (CAI). FTS, the key unit to retrieval atmospheric CO_2 and CH_4, observes sunlight reflected from the earth's surface and light emitted from the atmosphere and the surface. It has three narrow bands in the SWIR region (0.76, 1.6 and 2.0 μm) and a wide TIR band (5.5–14.3 μm) at spectral and spatial resolutions of 0.2 cm^{-1} and 10.5 km respectively [9]. CAI is employed to determine the cloud existence, aerosol loading and other states of the atmosphere over an extended area that includes the FTS's field of view (FOV) [8,9]. The measured information from CAI is used to correct the spectra obtained by FTS. To date, two typical CO_2 products have been generated from GOSAT, one is from the Japanese GOSAT team (hereafter called Japan-GOSAT product) [9] and the other is produced by the NASA's Atmospheric CO_2 Observations from Space (ACOS) team (hereafter called ACOS product) [3,13], both are collected here. The specific product versions used in this study are v01.1 and v2.0 for Japan-GOSAT product and v2.9 for ACOS product. All the products are with spatial resolution of 10.5 km.

1.3 SCIAMACHY

SCIAMACHY was successfully launched on board Environmental Satellite (ENVISAT) in 2002, which is a multichannel diode array satellite spectrometer covering the spectral range 0.24–2.38 μm with moderate spectral resolution of about 0.2–1.6 nm, and spatial resolution at nadir of 60 km×30 km [7]. It has eight spectral channels, with 1024 individual detector diodes for each band, observing simultaneously the spectral regions 0.24–1.75 μm (band 1–6), 1.94–2.04 μm (band 7) and 2.26–2.38 μm (band 8) in nadir and limb and solar and lunar occultation viewing geometries [14]. Detailed descriptions of SCIAMACHY can be found at [7,14]. Up to now, a number of CO_2 retrieval algorithms has been developed for SCIAMACHY [10,14–21], and two operational CO_2 products have been released by IUP/IFE of University of Bremen, i.e. WFM-DOAS product [14] and the Bremen Optimal Estimation DOAS (BESD) product [10,21]. Two versions of BESD product (v01.00.00 and v01.00.01) are employed in our study.

1.4 IASI

IASI is a key payload element of the METOP series of

European meteorological polar-orbit satellites. It was successfully launched on 19 October, 2006, and the second and third instruments will be mounted on the METOP-B and C satellites (http://smsc.cnes.fr/IASI/index.htm). IASI operates in the spectral range of 3.7–15.5 μm at a spectral resolution of 0.35–0.5 cm^{-1} [6]. The nominal footprint in nadir is about 12 km. The typical CO_2 retrieval algorithms can be found in [22,23]. In this study, the IASI CO_2 product is collected from NERC Earth Observation Data Centre (http://www.neodc.rl.ac.uk/browse/neodc/iasi/data/l2/).

1.5 Carbon Tracker (CT)

Carbon Tracker is a NOAA's data assimilation system which provides the 3D atmospheric profiles of CO_2 mole fractions over the globe. It forecasts atmospheric CO_2 mole fractions based on a combination of CO_2 surface exchange models (Ocean module, fire module, biosphere module, fossil fuel module, etc.) and an atmospheric transport model (Transport model 5 (TM5)) driven by meteorological fields from the European Centre for Medium-Range weather forecasts (ECMWF) [21,24]. In this study, Carbon Tracker data with version of CT2010 is collected. This dataset provides global CO_2 profiles with 3°×2° spatial grid and time interval of 3 h (total 8 times from 01 to 22 in UTC) spanning from January 2000 through December 2009. The CT dataset is used here mainly to assist the adjustment and spatiotemporal matching of those satellite-based CO_2 measurements. The characteristics of dataset employed in this study are summarized in Table 1.

2 Methods

2.1 Converting AIRS tropospheric CO_2 to XCO_2

As mentioned in section 1, AIRS as a TIR sounder, shows maximum sensitivity to atmospheric CO_2 in the middle to up troposphere, while other instruments, such as GOSAT and SCIAMACHY have a nearly uniform sensitivity to CO_2 from the surface up though the middle troposphere (thus are frequently used to derive XCO_2). It is generally hard to directly compare the AIRS tropospheric CO_2 to that of GOSAT and/or SCIAMACHY due to the different layers of the atmosphere they measured. For this point, a strategy has been suggested to convert tropospheric CO_2 to XCO_2 by incorporating the Carbon Tracker CO_2 profile and the averaging kernel of AIRS (eq. (1)).

$$\mathrm{AIRS}_{\mathrm{XCO_2}} = \frac{\omega^T x}{A^T x / \mathrm{sum}(A)} \times \mathrm{AIRS}_{\mathrm{CO_2}}, \quad (1)$$

where $\mathrm{AIRS}_{\mathrm{XCO_2}}$ is converted XCO_2 from AIRS tropospheric CO_2 product; $\mathrm{AIRS}_{\mathrm{CO_2}}$ is AIRS tropospheric CO_2 product; ω is pressure weighting function (N×1 matrix) for certain Carbon Tracker CO_2 profile; x is Carbon Tracker CO_2 profile (N×1 matrix) spatiotemporally collocated with AIRS retrieval; A is the averaging kernel vector of AIRS (N×1 matrix); The superscript T denotes the matrix transpose operation; sum(A) is the summation of the averaging kernel (Referred to the ATBD of AIRS CO_2 product at http://disc.sci.gsfc.nasa.gov/AIRS/documentation/AIRS-V5-Tropospheric-CO2-Products.pdf). Please note that, here, we just adopt the ratio of tropospheric CO_2 to column XCO_2 calculated from CT CO_2 profile using AIRS's averaging kernel, but not the absolute value of the CT profile. We assume that the ratio could, to some extent, depict the case of AIRS retrievals even if the CT profiles have a coarse spatial and vertical grid. If, however, CO_2 profiles with higher spatial and vertical resolutions can be available in the future, it is rarely a serious problem.

2.2 Converting IASI integrated CO_2 to XCO_2

Unlike AIRS, the publicly available CO_2 product from IASI (collected from the NERC Earth Observation Data Centre) is measured in column integrated CO_2 (kg/m^2) (according to IASI Level 2 Product Guide) despite the fact that it is also a TIR sounder. Likewise, it is difficult to inter-compare IASI-CO_2 product with that of other measurements due to the different units. Fortunately, IASI product released the surface pressure and atmospheric column specific humidity along with the CO_2 retrievals, which allow us to convert the integrated CO_2 to XCO_2 (eq. (2)).

$$\mathrm{IASI}_{\mathrm{XCO_2}} = \frac{\mathrm{Integrated\_CO_2} \times W \times g \times 10^6}{W_{\mathrm{CO_2}} \times P_{\mathrm{s}} \times \left(1 - w_{\mathrm{h2o}}\right)}, \quad (2)$$

where Integrated_CO_2 is the integrated CO_2 of IASI in units of kg/m^2; W is the molecular weight of dry air (28.99 g/mol);

Table 1 Characteristics of space-based CO_2 datasets used in this paper

Instruments or model	IFOV (km)	Overpass time	Spatial resolution of CO_2 product	Time Span (year 2009)	Version	Layer/column
AIRS	13.5	1:30 pm	90 km×90 km	12 months	v5	Tropospheric CO_2
GOSAT	10.5	1:00 pm	ACOS 10.5 km	Apr. –Dec.	v2.9	Column XCO_2
			Japan-GOSAT 10.5 km	Apr. –Dec.(v1.1) Jun. –Dec.(v2)	v1.1 & v2.0	
SCIAMACHY	60×30	10:00 am	60 km × 30 km	Jan. –Nov.	v01.00.00 & v01.00.01	Column XCO_2
IASI	12	9:30 am & pm	250 km (accuracy <20%)	12 months	–	Integrated CO_2, kg/m^2

W_{CO_2} is the molecular weight of CO_2 (44 g/mol); P_s is surface pressure (pa); w_{h2o} is atmospheric column specific humidity (kg/kg); g is gravitational acceleration (9.8 m/s^2).

2.3 Spatiotemporal matching and adjustments

To tackle different spatial samplings during comparison, the CO_2 retrievals with fine spatial resolutions are aggregated to a new value to match the relatively coarse scale retrieval considering their retrieval uncertainties. The smaller the uncertainty, the greater the weight is set.

Since different CO_2 retrievals have different overpass times, it is highly necessary to unify these times to avoid uncertainties induced by the time difference during the comparison. To this end, a method accounting for the CO_2 shift with time has been developed. Specifically, designate the GOSAT overpass time as reference, then transfer CO_2 measurements acquired at other times to that of the reference time by linearly interpolating the Carbon Tracker CO_2 profiles. Despite the fact that CO_2 absolute values of Carbon Tracker may not be accurate enough, here, the CO_2 daily cycle pattern it reflected is assumed to be correct.

Besides, it is not trivial to directly compare two CO_2 column retrievals (e.g. GOSAT and SCIAMACHY) due to the different averaging kernels and a priori CO_2 profiles they used. To allow the XCO_2 of GOSAT and SCIAMACHY to be physically comparable, the following equation is used to conquer this issue by adjusting these two measurements for a common a priori profile (i.e. the interpolated CT profile at the middle overpass time of the two XCO_2 retrievals being compared) [21,25].

$$X_{CO_2\_adj} = X_{CO_2\_ret} + \left(h^T I - a\right)\left(X_{CT} - X_a\right). \quad (3)$$

Here $X_{CO_2\_adj}$ is the adjusted XCO_2 for ACOS or BESD; $X_{CO_2\_ret}$ corresponds to retrieved XCO_2 of ACOS or BESD; a is column averaging kernel ($1\times N$ matrix) of ACOS or BESD; h is pressure weighting function ($N\times 1$ matrix). The superscript T denotes the transpose of h; I is an identity matrix; X_{CT} and X_a ($N\times 1$ matrix) are the common CT CO_2 profile and the corresponding *a priori* CO_2 profile for ACOS or BESD, respectively.

Up to now, theoretically, all CO_2 data collected in this study can be physically inter-compared by fully considering the above processes.

3 Results

3.1 Comparison of AIRS XCO_2 and tropospheric CO_2

To quantify the difference between the AIRS XCO_2 and tropospheric CO_2, the difference between the two variables (yearly mean CO_2 measurements) is calculated (Figure 1).

From Figure 1, we can see that at an annual scale, the difference between column and tropospheric CO_2 for AIRS is relatively small (less than 3 ppm). The regions of XCO_2 that are comparable or larger than that of troposphere are mainly occurred in the latitude band of 0°–35°N. The negative values are frequently detected in the difference map, which tells that the column measurements of CO_2 are not necessarily greater than that of tropospheric ones in magnitude although the CO_2 concentration at surface level is generally larger than that in the troposphere. We admit that some errors would be introduced if the CO_2 profiles used during the conversion are too smooth at vertical direction. However, this cannot deny the usefulness of the proposed converting strategy when the proper CO_2 profiles with higher vertical and spatial resolutions are available (for instance, the *in situ* profiles). Considering the high correlation and low bias between the AIRS XCO_2 and tropospheric CO_2 shown above, we directly employ the AIRS's tropospheric CO_2 in the subsequent analysis for convenience.

3.2 Correlation analyses

After applying the series processes described above, the CO_2 retrievals from SCIAMACHY, AIRS and GOSAT instruments are compared with that of ACOS considering the relatively high accuracy of ACOS [26]. We calculate the correlation coefficients and biases for each comparison. The relationships between different versions of CO_2 products for SCIAMACHY and GOSAT are also investigated. The scatter

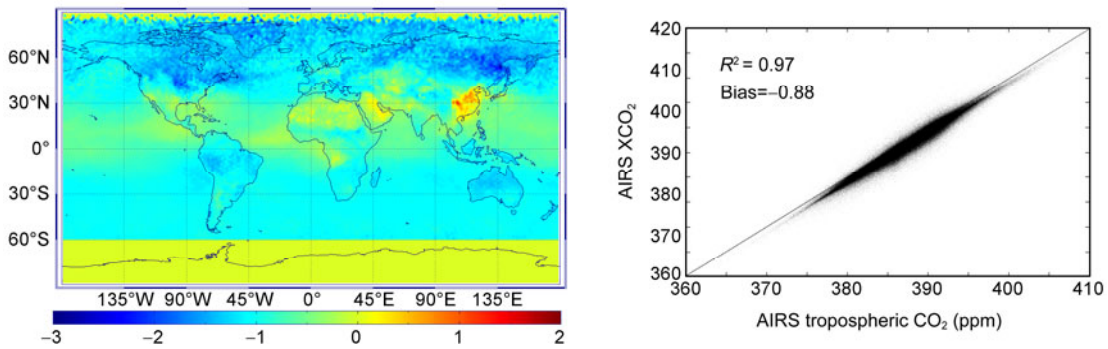

Figure 1 The global distribution of differences between AIRS XCO_2 and tropospheric CO_2 averaged in 1.5° by 1.5° bins (left) and their correlation(right).

diagrams are shown in Figure 2.

It can be seen from Figure 2 that ACOS XCO_2 shows the best agreement with that of Japan-GOSAT v2.0 product with the coefficient of determination (R^2) =0.783, followed by ACOS vs. BESD retrievals with R^2 greater than 0.3 for both versions of BESD products. In contrast, AIRS CO_2 shows a weak correlation with that of ACOS with R^2 less than 0.1. The reasons for that are probably contributed by: (1) Coarser scales of AIRS CO_2 product compared to that of GOSAT, so that some variations of CO_2 have been smoothed; (2) different atmospheric layers they detected. The signals sensed by AIRS mainly originated from the troposphere, while GOSAT shows a nearly uniform sensitivity to CO_2 in the whole atmosphere column. This implies the necessity to develop a robust method to transfer AIRS CO_2 to XCO_2; (3) some retrieval and processing errors.

On the global scale, XCO_2 retrievals from both AIRS and SCIAMACHY are higher in magnitude than that of ACOS with bias about 1.77 ppm for AIRS and 1.1–1.3 ppm for SCIAMACHY, while negative bias about −1.5 ppm is detected in Japan-GOSAT v2.0 product. The comparison of the two versions of Japan-GOSAT products indicates that the large negative bias (greater than 6 ppm) of XCO_2 has been removed in the newer version. Hence the XCO_2 retrievals from Japan-GOSAT gradually approach that of ACOS in the magnitude. Unlike the Japan-GOSAT data, the two BESD XCO_2 products show a very strong linear relationship, and the global bias between these two datasets is less than 1 ppm, which indicates the stability of the BESD algorithm.

Since valid IASI XCO_2 data are mainly distributed within the band of 50°–90°N (not shown here), which can rarely reflect the global CO_2 characteristics of IASI, the comparison of IASI against other products is temporarily not conducted here. The reason for that is still not fully understood.

3.3 Spatiotemporal characteristics of different space-based CO_2 datasets

As for the spatiotemporal characteristics of these products, the global distributions of XCO_2 are analyzed (Figures 3–7). For better visual appearance, the XCO_2 measurements have been averaged seasonally in 1.5° by 1.5° bins (Their original spatial scales can be found in Table 1). It should be noted that since the Japan-GOSAT v2.0 can only be available for June–December in 2009, thus the XCO_2 seasonal maps of summer, fall, winter plus a yearly mean (June–December) are shown in Figures 6 and 7. For better understanding the spatiotemporal features of these CO_2 products, some statistical data for yearly mean CO_2 are also given in Table 2.

From Figure 3, we can see that the XCO_2 of AIRS in

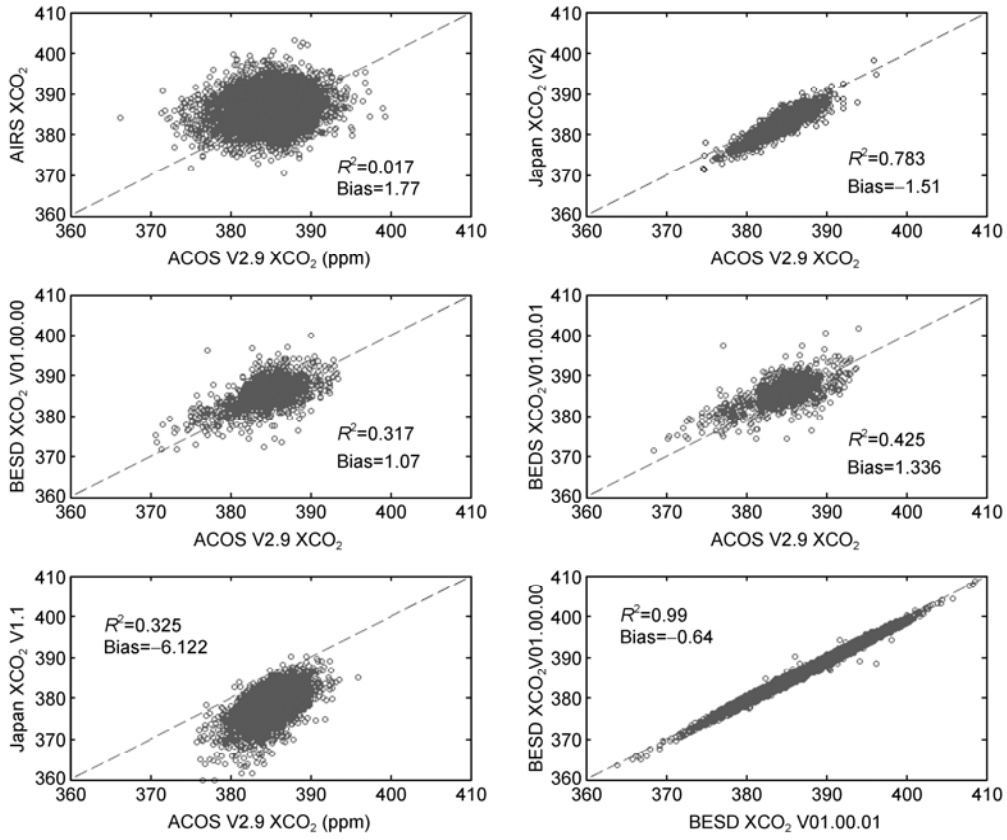

Figure 2 Scatter plots of ACOS XCO_2 versus that of AIRS, SCIAMACHY, and Japan-GOSAT, respectively over 2009.

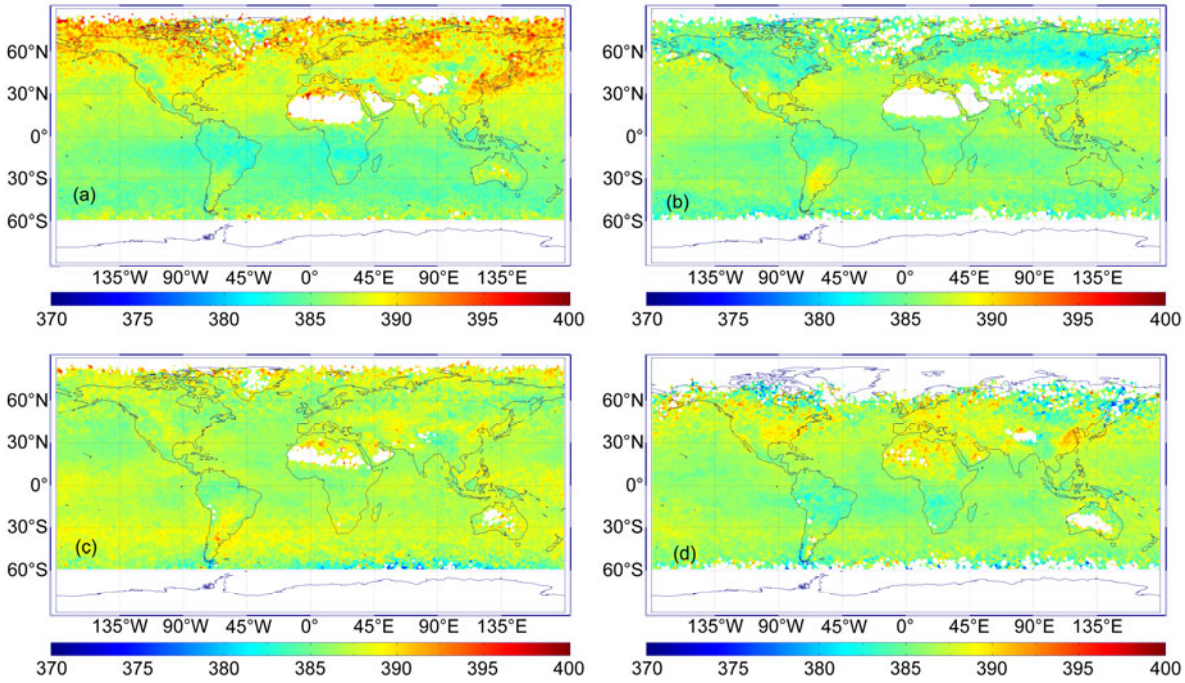

Figure 3 The global distribution of CO_2 averaged seasonally in 1.5° by 1.5° bins for AIRS in 2009. (a)–(d) indicate spring, summer, fall and winter respectively.

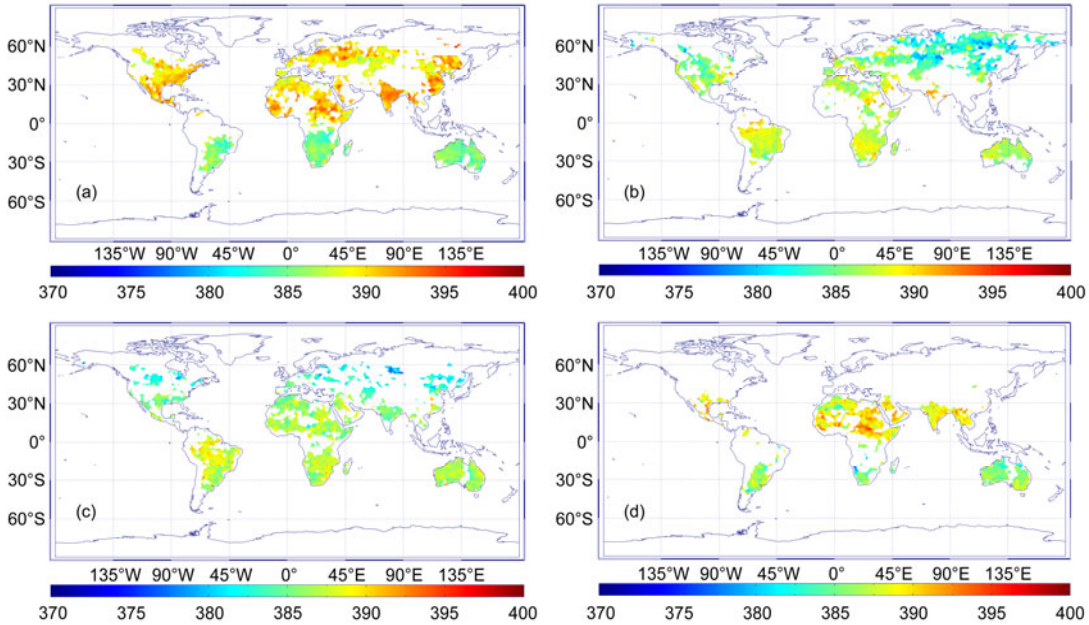

Figure 4 The global distribution of XCO_2 averaged seasonally in 1.5° by 1.5° bins for SCIAMACHY (BESD v01.001.01) in 2009. (a)–(d) indicate spring, summer, fall and winter (January and February only) respectively.

spring is generally higher than that of other seasons in the Northern Hemisphere due to the relatively weak plant photosynthesis, while no obvious seasonal variations in the Southern Hemisphere are observed. Similar seasonal variation can also be found in XCO_2 maps of SCIAMACHY and ACOS, apart from the sparse spatial coverage compared to AIRS (Figures 4–6). For global coverage, AIRS-CO_2 shows the largest spatial coverage. It is widely distributed within a range of 60°S–90°N. The valid XCO_2 data from SCIAMACHY are mainly restricted to land regions owing to the low signal-to-noise ratio over water bodies. While the XCO_2 derived from ACOS and Japan-GOSAT are distributed over both land and ocean areas. Even if over the land, the XCO_2 distribution of ACOS is slightly wider than that of SCIA-

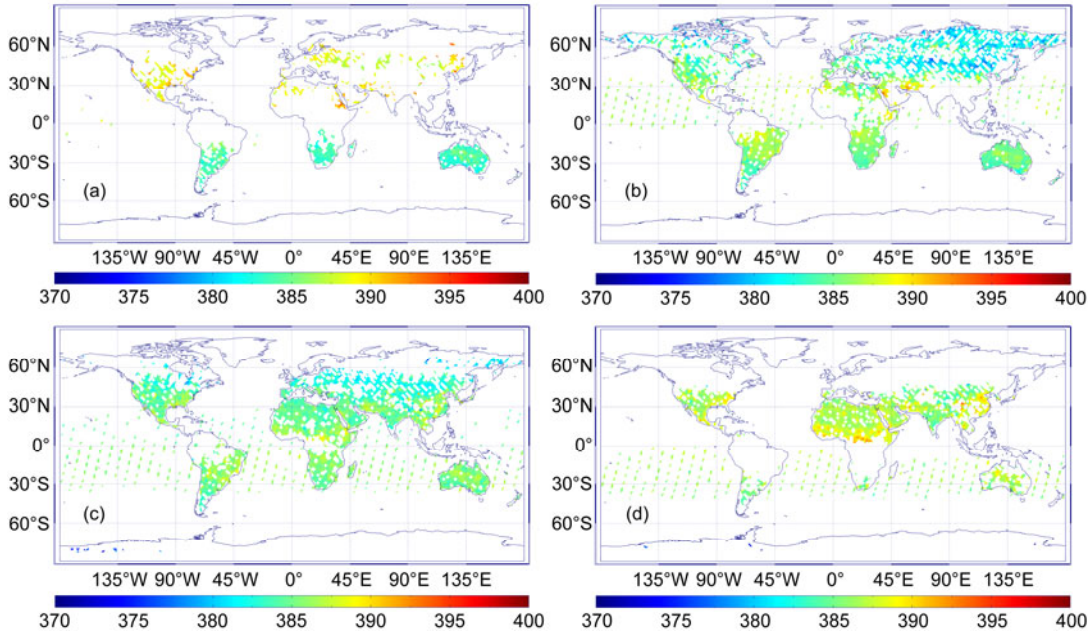

Figure 5 The global distribution of XCO_2 averaged seasonally in 1.5° by 1.5° bins for ACOS in 2009. (a)–(d) indicate spring (April and May), summer, fall and winter respectively.

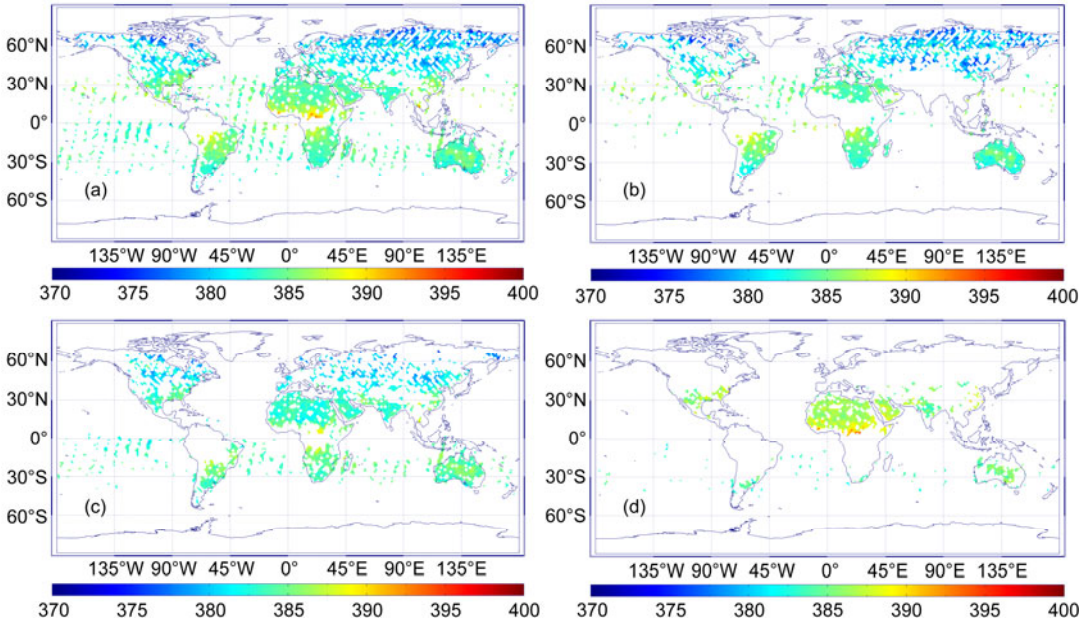

Figure 6 The global distribution of XCO_2 averaged seasonally in 1.5° by 1.5° bins for Japan-GOSAT v2.0 in 2009. (a)–(d) indicate yearly (June–December), summer, fall and winter, respectively.

MACHY. In contrast, the v1.1 version of Japan-GOSAT XCO_2 product shows the poorest global coverage. Furthermore, the XCO_2 concentration is uniformly low for all seasons with no noticeable seasonal variations even in the northern hemisphere. The Japan-GOSAT v2.0 product shows better agreement with ACOS in terms of both XCO_2 spatial coverage and seasonal variations. In addition, from Table 2 it is easy to tell that, all products show their maximum of standard deviation in the range of 60°–90°N, which, to some extent, implies relatively large CO_2 retrieval uncertainties within such area. On the whole, AIRS shows the smallest variation in all five latitude bands. Unlike AIRS, some variations in standard deviation can be detected in different latitude bands for other four products. Discrepancies can also be observed even within the same region for these CO_2 products. For spatial coverage, as shown above, AIRS possesses the largest and similar coverage in the five proposed regions, while for other datasets, larger coverage

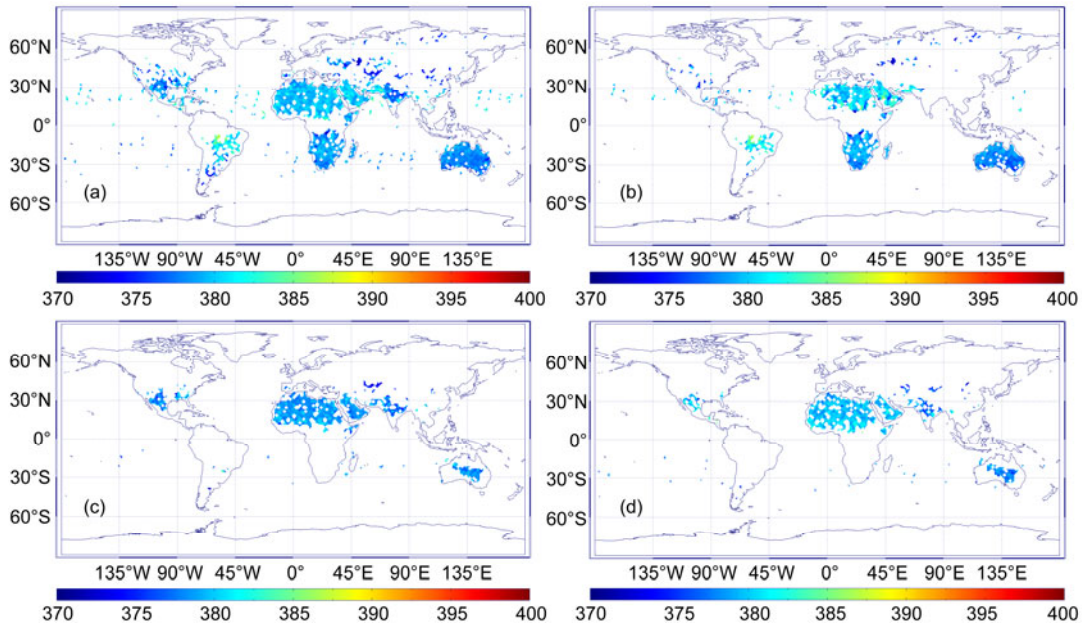

Figure 7 The global distribution of XCO_2 averaged seasonally in 1.5° by 1.5° bins for Japan-GOSAT v1.1 in 2009. (a)–(d) indicate yearly (June–December), summer, fall and winter, respectively.

Table 2 Spatial statistics of various CO_2 products within different latitude bands[a)]

CO_2 products		Latitude ranges				
		60°–90°N	30°–60°N	0°–30°N	0°–30°S	30°–60°S
AIRS	Mean	388.1	387.1	386.9	385.8	386.0
	Std.	3.1	1.1	1.0	0.76	1.0
	Coverage (%)	14.4	16.66	16.62	16.67	16.67
BESD v01.001.01	Mean	383.3	386.7	389.0	386.9	386.4
	Std.	4.1	3.0	2.0	1.5	1.9
	Coverage (%)	1.8	6.2	3.9	3.3	0.69
ACOS v2.9	Mean	381.6	384.6	386.2	385.9	385.3
	Std.	3.1	2.5	1.6	1.2	1.5
	Coverage (%)	3.5	7.5	6.7	6.8	2.2
Japan-GOSAT v2.0	Mean	379.2	382.3	385.2	384.3	383.1
	Std.	2.9	2.5	2.2	1.6	1.7
	Coverage (%)	3.0	6.45	5.65	6.3	2.1
Japan-GOSAT v1.1	Mean	376.0	377.6	380.0	378.8	377.5
	Std.	4.3	3.9	2.5	2.4	2.0
	Coverage (%)	0.68	2.9	4.6	3.4	1.0

a) CO_2 data within the region of 60°–90°S are not available for AIRS. Unit: ppm.

is frequently occurred within the region of 30°S–60°N.

Apart from the observing mechanism of the instruments, because the spatial resolutions of XCO_2 products from GOSAT (about 10.5 km) and SCIAMACHY (about 60 km× 30 km) are relatively higher than that of AIRS (about 90 km× 90 km), a great number of gaps are still exist in global maps of GOSAT and SCIAMACHY even if they are averaged in 1.5° by 1.5° bins. That is why the AIRS-XCO_2 maps seem smoother than other CO_2 maps. The complementarities of these CO_2 products in terms of spatial and temporal scales stimulate the study of their joint use.

In addition, the distribution pattern of atmospheric CO_2 along the latitude is also investigated. Initially the globe is divided into 8 sections according to the latitude at an interval of 20° from 90°N–60°S. For each section, the yearly mean XCO_2 is calculated, from which the distribution pat-

tern of the different XCO_2 products along the latitude is analyzed (Figure 8). It can be seen from Figure 8 that the latitudinal distribution of XCO_2 for ACOS, Japan-GOSAT and SCIAMACHY is very similar except for the overall difference of about 1–2 ppm between them. The CO_2 concentrations gradually ascend from the region of North Pole to the equator and then descend down to the South Pole, showing their higher concentration in the region of 30°N–30°S. While the CO_2 concentration of AIRS, as a whole, possess a uniformly descending trend from North to South Pole without showing perceptible latitudinal pattern.

4 Conclusion and discussions

The number of valid CO_2 measurements from a single space-based instrument is generally limited for certain day over a specific region due to the presence of clouds. The lack of sufficient data will definitely constrain the study of global CO_2 sources and sinks and data assimilation applications. Undoubtedly, it is a promising work to physically combine the currently available CO_2 products to generate an improved CO_2 dataset.

To this end, as a prerequisite, a series of strategies have been proposed in this study, including conversion of AIRS and IASI measurements to XCO_2 as well as spatiotemporal matching and adjustment. These suggested methods are proved to be very useful tools for making different CO_2 products spatiotemporally comparable. Based on these processes, global CO_2 retrievals of SCIAMACHY, AIRS and Japan-GOSAT product over 2009 are compared with that of ACOS (v2.9) considering the relatively high accuracy of ACOS. The results reveal that AIRS CO_2 measurements show a relatively weaker correlation with that of ACOS product with R^2 less than 0.1. The Japan-GOSAT v2.0 product shows the strongest correlation with that of ACOS (R^2 still less than 0.8 despite the fact that they originate from the same satellite) which is followed by BESD products. Global biases between these products are commonly less than 2 ppm, except a large negative bias for the v1.1 product of Japan-GOSAT. The inter-comparison of different versions of Japan-GOSAT as well as BESD products indicate that (1) the large global bias in CO_2 has been removed in the new version (v2.0) of Japan-GOSAT product; (2) the accuracy of the new product is very similar to that of ACOS except a negative bias of about −1.5 ppm globally; and (3) the two versions of BESD products show extremely high consistency which implies the stability of the BESD algorithms.

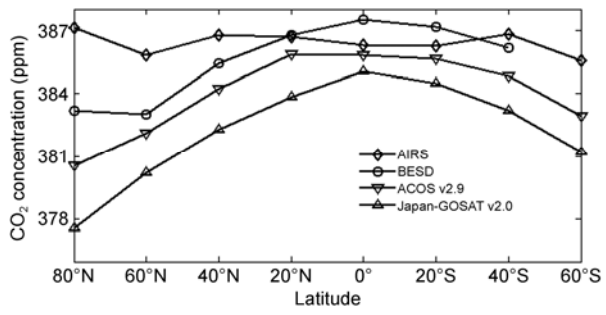

Figure 8 Latitudinal distributions of yearly averaged CO_2 for AIRS, ACOS, Japan-GOSAT and SCIAMACHY over 2009 (June–November).

On the whole, the CO_2 products from AIRS, SCIAMACHY, ACOS and Japan-GOSAT v2.0 show similar seasonal variation over global scale, while the spatial coverage of these products, except the AIRS data, is limited due probably to their relatively high spatial resolutions compared to that of AIRS. This can be evidenced by the vast gaps in the CO_2 maps of SCIAMACHY, ACOS and Japan-GOSAT v2.0 even aggregated in 1.5° by 1.5° bins. Specially, the v1.1 version of Japan-GOSAT product shows the poorest global coverage and no obvious CO_2 seasonal variation is detected. For SCIAMACHY, nearly no discrepancy can be found in the two versions of CO_2 products in terms of both XCO_2 coverage and seasonal variation. Moreover, all five datasets show their maximum of standard deviation in the range of 60°–90°N and some variations in standard deviation can be detected in different latitude bands. Discrepancies can also be observed even within the same region for these CO_2 products. Except for AIRS, larger coverage can be mostly occurred within the region of 30°S–60°N. As for the latitudinal distribution, an apparent arch-shaped pattern along latitude for ACOS, Japan-GOSAT and SCIAMACHY is detected, while no distinct latitudinal variation can be observed for AIRS. One point need to tell here is that the valid IASI CO_2 measurements are mainly restricted to areas of 50°–90°N, the reason for that is still under investigation. Considering its lack of representativeness of global CO_2 characteristics of IASI, the comparison and analyses associated with IASI are temporarily not conducted in this paper.

Although the current space-based CO_2 measurements could, to a certain extent, enhance our knowledge on global CO_2 sources and sinks, it is urgent for us to understand the remaining differences among these products in the near future. The present comparison analyses also imply that it is greatly necessary to improve and/or develop effective algorithms to better constrain the uncertainties when retrieving CO_2 from space. Considering the spatial coverage differences of these products, it is highly promising to combine such products to generate consistent products with improved spatial and temporal continuities. We admit that some errors may be introduced in the processes of CO_2 converting and spatiotemporal matching due to the relatively coarse grid of Carbon Tracker. This however is rarely a serious problem as long as CO_2 profiles with higher spatiotemporal and vertical resolutions can be available. At least, in this paper, we provide a series of possible strategies for physically comparing those available CO_2 products. Last point need to address is that the solutions proposed in this

paper are not restricted to CO_2 compression; instead they can be adapted to inter-compare retrievals of other trace gaseous as well as profiles of atmospheric temperature, water vapor, etc.

This work was supported by the Strategic Priority Research Program (*XDA05040402*) *and the CAS/SAFEA International Partnership Program for Creative Research Teams* (*KZZD-EW-TZ-09*). *Many thanks are given to SCIAMACHY Team at University of Bremen IUP/IFE as well as AIRS, GOSAT and IASI scientific teams for providing us the CO_2 products. We also thank the anonymous reviewers for their valuable comments to improve this work.*

1 Morino I, Uchino O, Inoue M, et al. Preliminary validation of column-averaged volume mixing ratios of carbon dioxide and methane retrieved from GOSAT short-wavelength infrared spectra. Atmos Meas Tech, 2011, 4: 1061–1076
2 Butz A, Hasekamp O P, Frankenberg C, et al. Retrievals of atmospheric CO_2 from simulated space-borne measurements of backscattered near-infrared sunlight: Accounting for aerosol effects. Appl Opt, 2009, 48: 3322–3336
3 O'Dell C W, Connor B, Bösch H, et al. The ACOS CO_2 retrieval algorithm–Part 1: Description and validation against synthetic observations, Atmos Meas Tech, 2012, 5: 99–121
4 Gautier C, Shiren Y, Hofstadter M D. AIRS Vis/Near IR instrument. IEEE Trans Geosci Remote Sensing, 2003, 41: 330–342
5 Chahine M T, Gautier C, Goldberg M D, et al. AIRS/AMSU/HSB on the Aqua mission: Design, science objectives, data products, and processing systems. IEEE Trans Geosci Remote Sensing, 2003, 41: 253–264
6 Phulpin T, Cayla F R, Chalon G, et al. IASI on board Metop: Project status and scientific preparation, paper presented at 12th International TOVS Study Conference, Lorne, Vi ctoria, Australia, 2002
7 Bovensmann H, Burrows J P, Buchwitz M, et al. SCIAMACHY—Mission objectives and measurement modes. J Atmos Sci, 1999, 56: 127–150
8 Kuze A, Suto H, Nakajima M, et al. Thermal and near infrared sensor for carbon observation Fourier-transform spectrometer on the Greenhouse Gases Observing Satellite for greenhouse gases monitoring. Appl Opt, 2009, 48: 6716–6733
9 Yokota T, Yoshida Y, Eguchi N, et al. Global Concentrations of CO_2 and CH_4 Retrieved from GOSAT: First Preliminary Results, SOLA, 2009, 5: 160–163
10 Reuter M, Buchwitz M, Schneising O, et al. A method for improved SCIAMACHY CO_2 retrieval in the presence of optically thin clouds. Atmos Meas Tech, 2010, 3: 209–232
11 Crisp D, Atlas R M, Breon F M, et al. The Orbiting Carbon Observatory (OCO) mission. Adv Space Res, 2004, 34: 700–709
12 Chahine M, Barnet C, Olsen E T, et al. On the determination of atmospheric minor gases by the method of vanishing partial derivatives with application to CO_2. Geophys Res Lett, 2005, 32: 1–5
13 Crisp D, Fisher B M, O'Dell C, et al. The ACOS XCO_2 retrieval algorithm, Part 2: Global XCO_2 data characterization. Atmos Meas Tech, 2012, 5: 1–60
14 Buchwitz M, Rozanov V V, Burrows J P. A near-infrared optimized DOAS method for the fast global retrieval of atmospheric CH_4, CO, CO_2, H_2O, and N_2O total column amounts from SCIAMACHY Envisat-1 nadir radiances. J Geophys Res, 2000, 105: 15231–15245
15 Buchwitz M, Beek R, Burrows J P, et al. Atmospheric methane and carbon dioxide from SCIAMACHY satellite data: Initial comparison with chemistry and transport models. Atmos Chem Phys, 2005, 5: 941–962
16 Buchwitz M, Beek R de, Noël S, et al. Carbon monoxide, methane and carbon dioxide columns retrieved from SCIAMACHY by WFM-DOAS: Year 2003 initial data set. Atmos Chem Phys, 2005, 5: 3313–3329
17 Houweling S, Hartmann W, Aben I, et al. Evidence of systematic errors in SCIAMACHY-observed CO_2 due to aerosols. Atmos Chem Phys, 2005, 5: 3003–3013
18 Barkley M P, Frieβ U, Monks P S. Measuring atmospheric CO_2 from space using Full Spectral Initiation (FSI) WFM-DOAS. Atmos Chem Phys, 2006, 6: 3517–3534
19 Bösch H, Toon G C, Sen B, et al. Space-based near-infrared CO_2 measurements: Testing the orbiting carbon observatory retrieval algorithm and validation concept using SCIAMACHY observations over Park Falls, Wisconsin. J Geophys Res, 2006, 111: d23302
20 Schneising O, Buchwitz M, Burrows J P, et al. Three years of greenhouse gas column-averaged dry air mole fractions retrieved from satellite-Part 1: Carbon dioxide. Atmos Chem Phys, 2008, 8: 3827–3853
21 Reuter M, Bovensmann H, Buchwitz M, et al. Retrieval of atmospheric CO_2 with enhanced accuracy and precision from SCIAMACHY: Validation with FTS measurements and com-parison with model results. J Geophys Res, 2011, 116: D04301
22 Turquety S, Hadji-Lazaro J, Clerbaux C, et al. Operational trace gas retrieval algorithm for the infrared atmospheric sounding interferometer. J Geophys Res, 109: D21301
23 Schlüssel P, Hultberg T H, Phillips P L, et al. The operational IASI Level 2 processor. Adv Space Res, 2005, 36: 982–988
24 Peters W, Jacobson A R, Sweeney C, et al. An atmospheric perspective on North America carbon dioxide exchange: Carbon Tracker. Proc Natl Acad Sci USA, 2007, 104: 18925–18930
25 Rodgers C D. Inverse Methods for Atmospheric Sounding: Theory and Practice. Singapore: World Scientific Publishing Co. Ltd., 2000
26 Wunch D, Wennberg P O, Toon G C, et al. A method for evaluating bias in global measurements of CO_2 total columns from space. Atmos Chem Phys, 2011, 11: 12317–12337